Poly(trimethylene terephthalate) Nanocomposite Fibers Comprising Different Organoclays: Thermomechanical Properties and Morphology

Jin-Hae Chang,[1] Mu Kyung Mun,[1] Jeong-Cheol Kim[2]

[1]*Department of Polymer Science and Engineering, Kumoh National Institute of Technology, Gumi 730-701, Korea*
[2]*Gwangju R&D Center, Korea Institute of Industrial Technology, Gwangju 500-460, Korea*

Received 2 January 2006; accepted 25 April 2006
DOI 10.1002/app.24948
Published online in Wiley InterScience (www.interscience.wiley.com).

ABSTRACT: Poly(trimethylene terephthalate) (PTT) nanocomposites were synthesized by *in situ* polymerization at high temperature with two thermally stable organoclays: 1,2-dimethylhexadecylimidazolium-montmorillonite (IMD-MMT) and dodecyltriphenyl phosphonium-MMT (C_{12}PPh-MMT). PTT hybrid fibers with various organoclay contents were melt-spun at various draw ratios (DRs) to produce monofilaments. The thermomechanical properties and morphologies of the PTT hybrid fibers were characterized using differential scanning calorimetry, thermogravimetric analysis, wide-angle X-ray diffraction, electron microscopy, and mechanical tensile properties analysis. The nanostructure of the hybrid fibers was observed by both scanning and transmission electron microscopy, which showed that the clay layers were well dispersed into the matrix polymer, although some clusters or agglomerated particles were also detected. Unlike the hybrids containing IMD-MMT, the clay layers of the C_{12}PPh-MMT hybrid fiber were more dispersed into the matrix polymer. The thermal stability and tensile properties of the hybrid fibers increased with increasing clay content for DR = 1. However, as DR increased from 1 to 9 the ultimate strength and initial modulus of the hybrid fibers with IMD-MMT increased slightly whereas those of C_{12}PPh-MMT hybrid fibers decreased slightly. © 2006 Wiley Periodicals, Inc. J Appl Polym Sci 102: 4535–4545, 2006

Key words: polyester; nanocomposites; organoclay; fibers

INTRODUCTION

Polymeric nanocomposites are a class of composites consisting of ultrafine inorganic particles with sizes on the order of nanometers that are homogeneously dispersed in a polymer matrix. The nanosize of the particles means that nanocomposites possess mechanical properties that are superior to those of conventional composites because interfacial adhesion is maximized.[1–3]

Nano-scale composites of polymers with clays or organoclays are receiving considerable attention, with both intercalated and exfoliated nanocomposites being prepared using several preparation methods.[4–6] The three most commonly used methods are polymer solution intercalation, polymer melt intercalation, and monomer intercalation *in situ* polymerization in which monomers are intercalated into the clay galleries followed by polymerization. The last production method relies on swelling of the organoclay by the monomer, followed by *in situ* polymerization initiated thermally or by the addition of a suitable compound. The chain growth in the clay galleries accelerates clay exfoliation and nanocomposite formation. This technique of *in situ* interlayer polymerization is also particularly attractive because of its versatility and compatibility with reactive monomers, and is beginning to be used in commercial applications.[7–10]

Poly(trimethylene terephthalate) (PTT) is an aromatic polyester made from the polycondensation of 1,3-propanediol (PDO) and a terephthalic acid, and was first reported by Whinfield and Dickson in 1941.[11,12] PTT has found many applications in fibers, injection molding, and film production, and offers good tensile behavior, outstanding elastic recovery, and dyeability. Moreover, PTT fibers have the resiliency and softness of nylon fibers, as well as the chemical stability and stain resistance of their poly(ethylene terephthalate) (PET) counterparts, making them ideal candidates for use in applications such as carpets and other textile fibers. The low moisture absorption and fiber modulus of PTT endows carpets with a desirable dry and soft feel.[13–16]

The preparation of PTT nanocomposites requires elevated temperatures (>265°C) for *in situ* intercalation and bulk processing. Decomposition will occur if the processing temperature is higher than the thermal

Correspondence to: J.-H. Chang (changjinhae@hanmail.net).
Contract grant sponsor: Kumoh National Institute of Technology.

stability of the organoclay, altering the interface between the filler and the matrix polymer. In real processes with organophilic polymers, the interlayer cations are replaced with alkyl ammonium cations to enhance the dispersibility. Many research groups have extensively studied the preparation of organoclays with more stable thermal properties.[17–20]

The present study evaluated the effects of varying the amount of organoclay and different draw ratios (DRs) on the properties of the PTT hybrid fibers. To obtain nanocomposites without producing thermal degradation during processing, we used two thermally stable organoclays: 1,2-dimethylhexadecylimidazolium-montmorillonite (IMD-MMT) and dodecyltriphenyl phosphonium-MMT (C_{12}PPh-MMT). The effects of these organoclays on the thermal stability, tensile properties, and morphology of the resulting hybrid fibers were also examined. In this article we describe the method used to fabricate PTT nanocomposites, which used *in situ* intercalation polymerization. The properties of IMD-MMT/PTT hybrid fibers were compared with those of fibers prepared from C_{12}PPh-MMT/PTT hybrids using differential scanning calorimetry (DSC), thermogravimetric analysis (TGA), wide-angle X-ray diffraction (XRD), scanning electron microscopy (SEM), transmission electron microscopy (TEM), and tensile properties testing.

EXPERIMENTAL

Materials

The source clay, Kunipia-F (Na^+-MMT), was obtained from Kunimine Industry Co. (Tokyo, Japan), and was screened with a 325-mesh sieve to obtain clay with a cationic-exchange capacity of 119 mequiv./100 g. With the exception of PDO (Shell Co., USA), all reagents were purchased from TCI and Aldrich Chemical Co. Commercially available solvents were purified by distillation, and common reagents were used without further purification.

Syntheses of the PTT nanocomposites

The two types of organically modified clays (IMD-MMT and C_{12}PPh-MMT) used in this study were synthesized using an ion-exchange reaction between Na^+-MMT and IMD-Cl^- and between Na^+-MMT and C_{12}PPh-Cl^-, respectively. The two organophilic clays were obtained through a multistep process using methods that we have described previously.[10] The chemical structures of the organoclays are shown in Scheme 1.

Since we used very similar procedures to synthesize IMD-MMT/PTT and C_{12}PPh-MMT/PTT, only the preparation of the PTT nanocomposite containing 2 wt % IMD-MMT is described here. PDO (76.0 g, 1.0 mol) and 2.08 g of IMD-MMT were placed in a polymerization tube and stirred for 30 min at room temperature. In a separate tube, dimethyl terephthalate (DMT) (97.0 g, 0.5 mol) and a few drops of isopropyl titanate (1.2×10^{-4} mol) were mixed together and then added to the organoclay-PDO system with vigorous stirring to obtain a homogeneously dispersed system. The resulting mixture was then first heated at 190°C for 1 h, after which the temperature was raised to 230°C and the mixture stirred for a further 2 h under a steady stream of N_2 gas. Methanol was generated continuously during this period. In the final step, the mixture was heated at 265°C for a further 2 h at a pressure of 1 Torr.

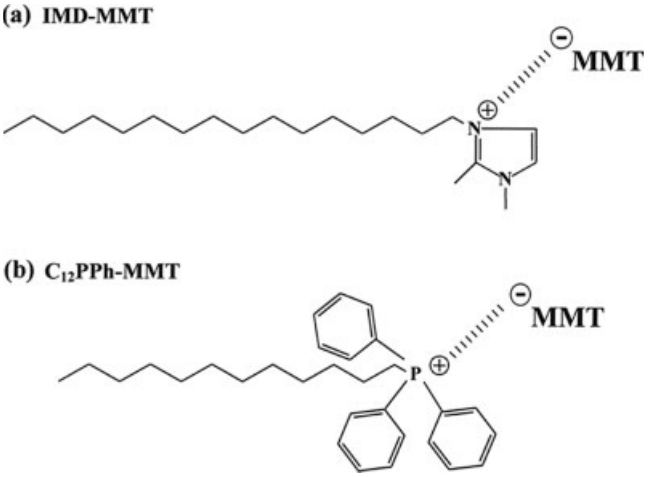

Scheme 1 Chemical structures of organoclays.

The crude solid was washed repeatedly with water and then dried under a vacuum at 70°C for 24 h to produce the IMD-MMT/PTT nanocomposites. The solution viscosity of the organoclay/PTT nanocomposites was studied in 50/50 (w/w) phenol-1,1,2,2-tetrachloroethane. The inherent viscosities of the samples were unchanged by the processing performed in the study (Table I). We attempted to synthesize PTT hybrids containing more than 3 wt % organoclay using the *in situ* intercalation approach. However, repeated attempts to polymerize a 4 wt % IMD-MMT hybrid all failed because of the production of bubbles in the polymerization reactor during the transesterification of DMT and PDO. The problem of how to produce high-molecular-weight polymer hybrids with a high organoclay content without the formation of bubbles remains unresolved (we are currently investigating this further).

Extrusion

The PTT hybrids were compressed (2500 kg/cm^2) for 2–3 min on a hot press at 250°C. The resulting films ($\sim$ 0.5 mm thick) were then dried in a vacuum oven at 110°C for 24 h, and extruded through the die of a capillary rheometer (model 5460, Instron) at 250°C. The

TABLE I
Thermal Properties of PTT Hybrid Fibers

Organoclay (wt %)	DR[a]	IMD-MMT				C_{12}PPh-MMT			
		IV[b]	T_m (°C)	T_D^{ic} (°C)	wt_R^{600d} (%)	IV	T_m (°C)	T_D^i(°C)	wt_R^{600} (%)
0 (pure PTT)	1	0.84	228	362	1	0.84	228	362	1
1	1	0.81	232	367	8				
2	1	0.80	232	370	10	0.86	227	371	10
3	1	0.85	232	372	11	0.83	228	370	11
	3		233	371	11				
	7		232	372	10				
	9		232	371	10				
4	1					0.81	227	371	12
	3						228	370	12
	7						227	370	13
	9						228	371	13

[a] Draw ratio.
[b] Inherent viscosities were measured at 30°C by using 0.1 g/100 mL solutions in a phenol/1,1,2,2-tetrachloroethane (50/50 = w/w mixture.
[c] Initial weight-loss onset temperature.
[d] Weight percent of residue at 600 °C.

hot extrudates were immediately drawn through a capillary die at constant speed to form fibers with different DRs, where the standard die diameter was 0.75 mm. The DR values were calculated from the ratio of the velocity of extrusion to the take-up speed, where the mean time within the capillary rheometer was 3–4 min. The take-up speeds depended on the viscosity, matrix polymers, filler concentration of the matrix polymer, and the like.

Characterization

The thermal behavior of the PTT hybrids was studied using combined DSC (model 910, DuPont) and TGA, at a heating rate of 20°C/min under a steady stream of N_2 gas. The weight residue at 600°C was determined as the ashes remaining when the sample was heated to 600°C. XRD measurements were performed at room temperature using an X-ray diffractometer (D/Max-IIIB, Rigaku) with Ni-filtered Co-Kα radiation. The scanning was conducted with 2θ ranging from 2° to 10°, at a rate of 2°/min.

The tensile properties of the as-produced PTT hybrid fibers were determined at room temperature using a mechanical tester (model 5564, Instron) with a crosshead speed of 20 mm/min. The experimental uncertainties in the ultimate strength and initial modulus were determined from more than 10 independent measurements: they were ±1 MPa and ±0.05 GPa, respectively.

The morphologies of the fractured extruded fiber surfaces were investigated using SEM (model S-2400, Hitachi). An SPI sputter coater was used to sputter the fractured surfaces with gold so as to enhance their conductivity. The samples for TEM were prepared by placing the PTT hybrid fibers into epoxy capsules and then curing the epoxy at 70°C for 24 h under reduced pressure. The cured epoxies were then microtomed (~ 90 nm thick), and a layer of carbon (~ 3 nm) was

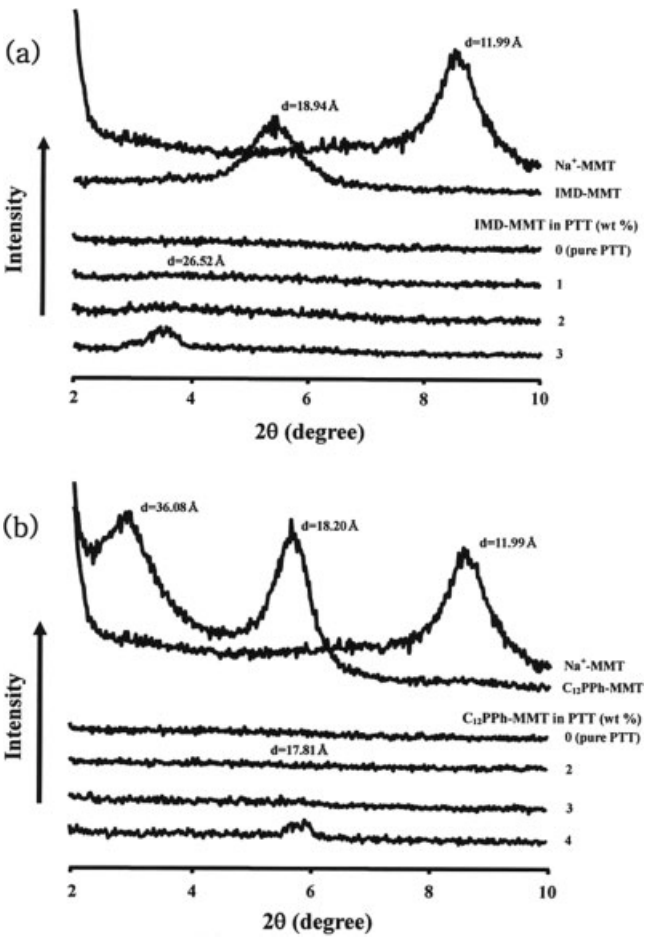

Figure 1 XRD patterns for clay, organoclays, and PTT hybrid fibers with various organoclay contents.

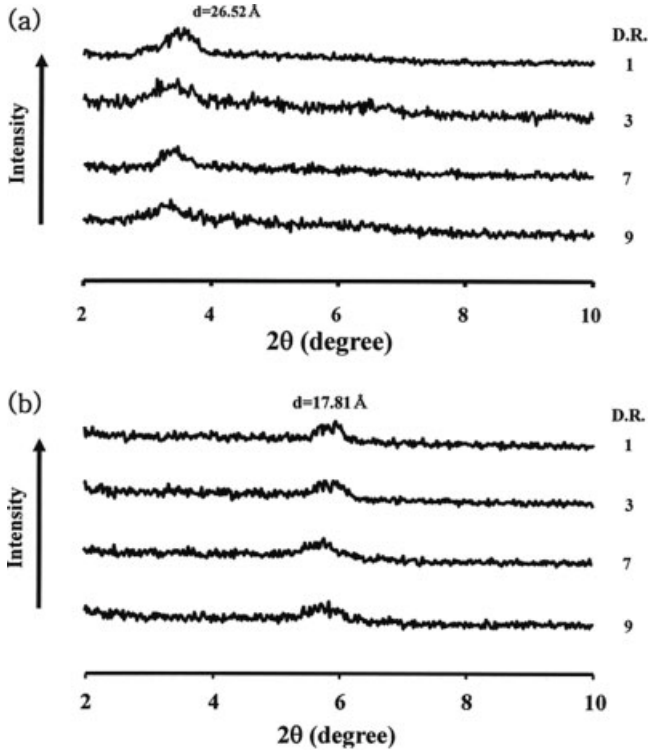

Figure 2 XRD patterns of (a) 3 wt % IMD-MMT and (b) 4 wt % C_{12}PPh-MMT in PTT hybrid fibers with different draw ratios.

deposited on each of the slices, which were subsequently placed on copper grids (mesh 200). TEM photographs of the ultrathin polymer/organoclay hybrid sections were taken (model EM 912, OMEGA) at an acceleration voltage of 120 kV.

RESULTS AND DISCUSSION

Wide-angle X-ray diffraction

The X-ray diffractograms of pure PTT, the organoclays, and organoclay/PTT hybrid fibers are shown in Figure 1. The d_{001} reflection for the Na^+-MMT occurred at $2\theta = 8.60^\circ$, which corresponds to an interlayer spacing (d) of 11.99 Å. The XRD peak for the surface-modified clay, IMD-MMT, occurred at $2\theta = 5.42^\circ$, corresponding to $d = 18.94$ Å [Fig. 1(a)]. The clays modified with an organic compound exhibited improved compatibility with the polymer, enabling the clay galleries to be easily intercalated with the polymer. As expected, the ion exchange between the clay (Na^+-MMT) and IMD^+-Cl^- resulted in an increase in the basal interlayer spacing with respect to that of pristine Na^+-MMT and in a large shift of the diffraction peak toward lower values of 2θ. For the PTT with an organoclay content of 1 wt %, only a slight peak at $2\theta = 3.87^\circ$ ($d = 26.52$ Å) was evident in the XRD results for the fiber sample.

In the case of C_{12}PPh-MMT [Fig. 1(b)], ion exchange between the Na^+-MMT and the C_{12}PPh-Cl^- also caused a large shift of the diffraction peak toward lower values of 2θ. The interlayer spacing of C_{12}PPh-MMT ($d = 36.08$ Å) was larger than that of IMD-MMT ($d = 18.94$ Å). Obvious clay peaks appeared in the XRD curves of the PTT hybrid fibers with 2–4 wt % organoclay, which indicates that the clay layers of the organoclays were intercalated (not exfoliated) and not homogeneously dispersed in the PTT matrix. A sec-

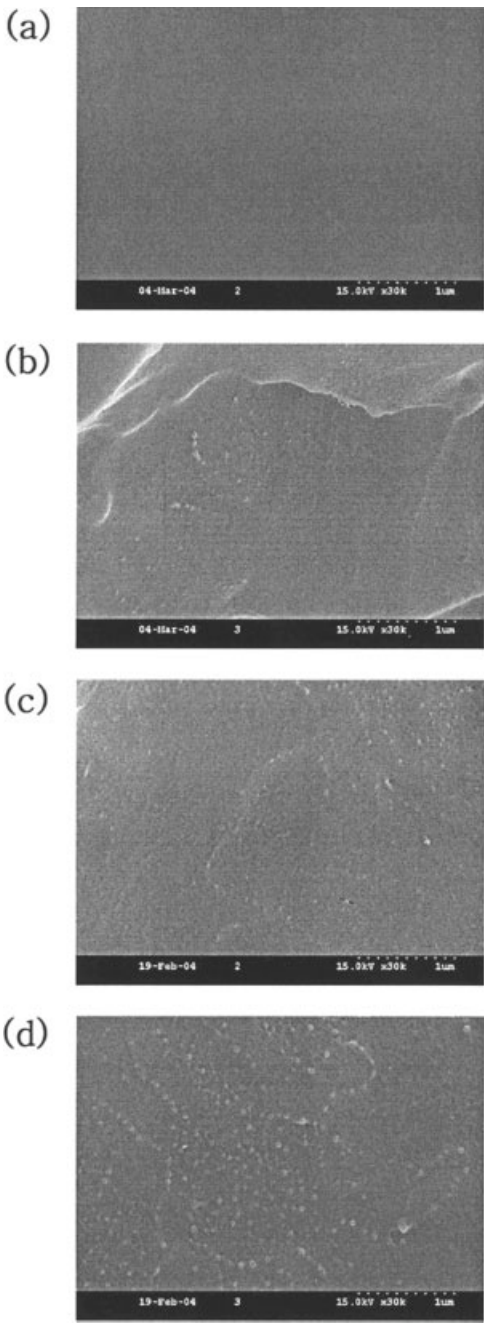

Figure 3 SEM photographs of (a) 0 wt % (pure PTT), (b) 1 wt %, (c) 2 wt %, and (d) 3 wt % IMD-MMT in PTT hybrid fibers.

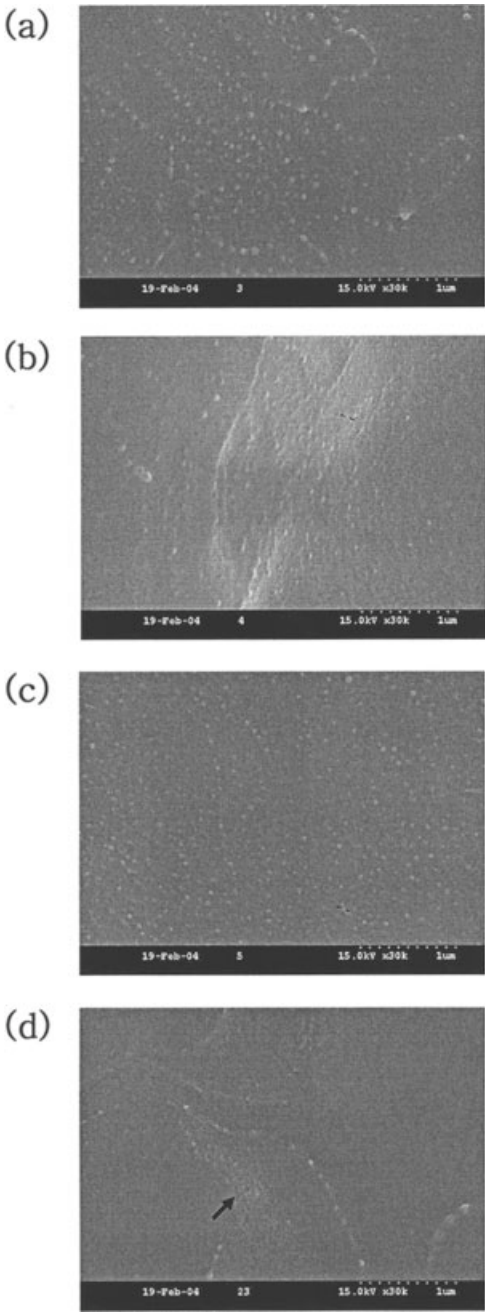

Figure 4 SEM photographs of 3 wt % IMD-MMT in PTT hybrid fibers for draw ratios: (a) 1, (b) 3, (c) 7, and (d) 9.

ond XRD peak was also observed at $2\theta = 5.65^\circ$ ($d = 18.20$ Å), which correlates to the (002) plane of the organoclay layers.

The interlayer spacing was larger for the hybrids than for the pristine organoclays. After intercalation by the organoclays, d increased from 11.99 to 18.94 Å ($2\theta = 5.42^\circ$) for the IMD-MMT hybrid fiber and from 11.99 to 36.08 Å ($2\theta = 2.86^\circ$) for the C_{12}PPh-MMT hybrid fiber. This increase in the basal spacing indicates the intercalation of the polymer chains into the clay galleries.[21,22] Increases in the amount of organoclay in the PTT matrices resulted in the appearance of sharp peaks in this region, whose intensities increased linearly with the clay content [Fig. 1(a,b)]. This suggests that some portions of the organoclay aggregated, and that the dispersion was better at a lower clay content than at a higher clay content. However, the presence of the organoclay had no effect on the locations of the peaks, which indicates that perfect exfoliation of the layering of clay in the organoclay does not occur in PTT.[23] For PTT hybrid fibers, the disappearance of the main peaks (at $2\theta = 5.42^\circ$ for IMD-MMT and at $2\theta = 2.86^\circ$ for C_{12}PPh-MMT) was attributed to the swollen organoclay inserted when the polymer chains exhibited a diffraction peak lower than 2°.[24]

Figure 2(a,b) show the XRD results for the PTT hybrid fibers containing 3 wt % IMD-MMT and 4 wt % C_{12}PPh-MMT, respectively, for various values of DR. When DR = 1, peaks were present for both extruded fibers. Because stretching of the fibers increases the alignment of clay platelets in a polymer matrix, the peak intensity in XRD usually decreases

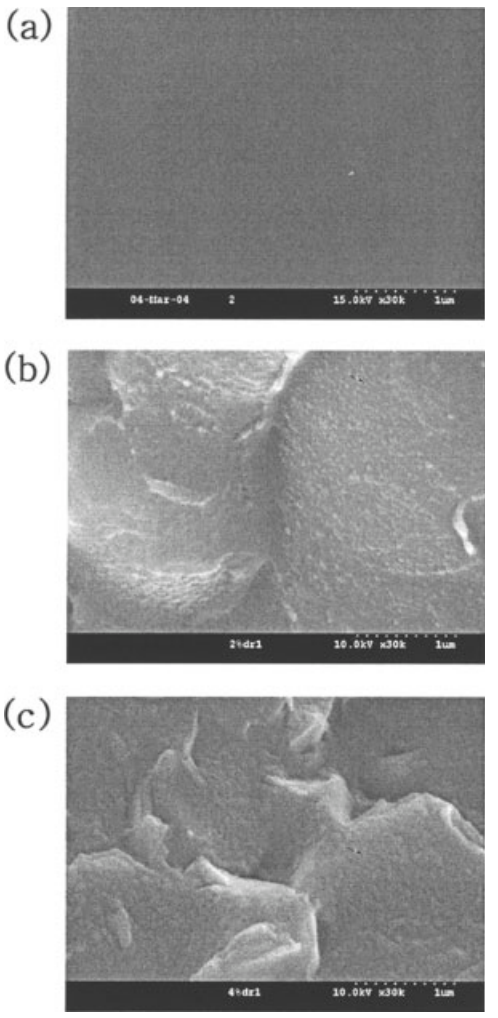

Figure 5 SEM photographs of (a) 0 wt % (pure PTT), (b) 2 wt %, and (c) 4 wt % C_{12}PPh-MMT in PTT hybrid fibers.

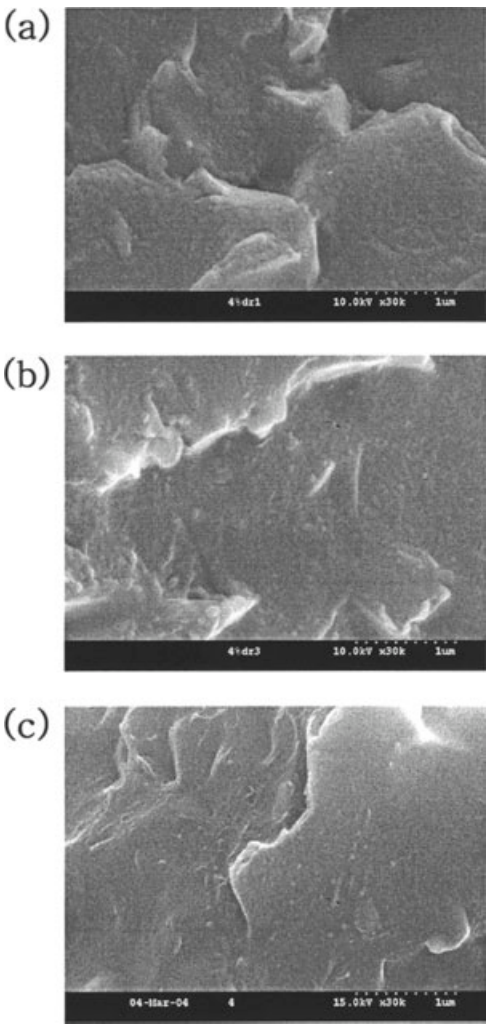

Figure 6 SEM photographs of 4 wt % C_{12}PPh-MMT in PTT hybrid fibers for draw ratios: (a) 1, (b) 3, and (c) 9.

with increasing DR in coil-like polymers.[10] However, significant decreases in the XRD peak intensities were not observed in either system when the DR was increased from 1 to 9, implying that higher stretching of the fiber during the extrusion was not effective for good dispersion of the clay in the polymer matrix. The DR values in these systems, however, had little effect on the peak position, which indicates that perfect exfoliation of the organoclay layer structure does not occur in PTT.

Morphology

XRD is by far the simplest method available for measuring the interlayer spacing of the hybrids. However, we extended this by using SEM and TEM to evaluate the degree of intercalation and the amount of aggregation of the clay clusters.

The morphology of the aggregated clay was characterized using SEM. Because of the difference in the scattering densities of clay and PTT, large clay aggregates were readily evident in SEM images. The SEM images of the fractured surfaces of the PTT hybrid fibers containing the two organoclays are compared in Figures 3–6. Figure 3 reveals that clay phases were formed within undrawn PTT hybrid fibers with increasing organoclay content (0–3 wt %). These PTT hybrid fibers consisted of clay domains that were 50–80 nm in size and dispersed in a continuous PTT phase. Figure 4 shows micrographs taken of the 3 wt % IMD-MMT/PTT hybrid fiber obtained for DRs from 1 to 9. When DR = 7, the 3 wt % hybrid fiber contained fine clay phases that were 50–60 nm in diameter [Fig. 4(c)], with the domains exhibiting very similar diameters (40–60 nm) for DR = 9 [Fig. 4(d)]. The domain size of the dispersed clay phase and the formed voids were virtually constant irrespective of DR, which is consistent with the XRD observations shown in Figure 2.

Figure 5 shows the clay phases formed in an undrawn hybrid fiber for organoclay from 0 to 4 wt %. The PTT hybrid fibers with 0–4 wt % C_{12}PPh-MMT consisted of clay domains with a size of 50–70 nm in a continuous PTT phase. The micrographs of the pure PTT [Fig. 5(a)] and the PTT hybrid fiber containing 2 wt % organoclay [Fig. 5(b)] reveal smooth surfaces due to better dispersion of the clay particles. Con-

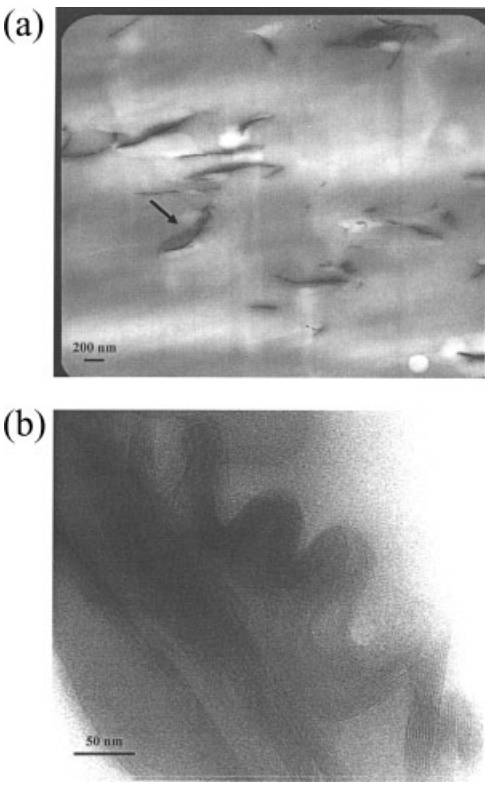

Figure 7 TEM micrographs of 1 wt % IMD-MMT in PTT hybrid fiber increasing the magnification levels from (a) to (b).

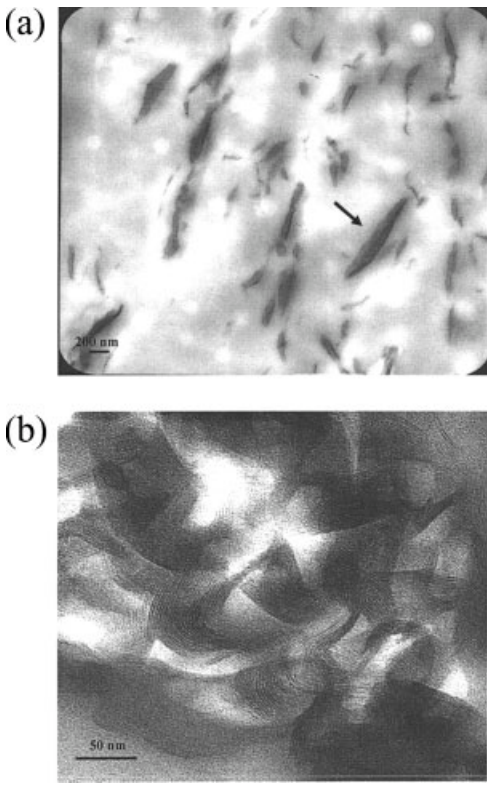

Figure 8 TEM micrographs of 3 wt % IMD-MMT in PTT hybrid fiber at two different magnification levels.

versely, Figure 5(c) shows voids and some deformed regions that may be attributable to the coarseness of the fractured surface. However, the fractured surfaces were more deformed when the hybrids contained more organoclay, which is probably a consequence of the agglomeration of clay particles.

Figure 6 shows micrographs of the 4 wt % C_{12}PPh-MMT/PTT hybrid fiber for different DRs. The domain size of the organoclay remained virtually unchanged for DR from 1 to 9. The hybrid fiber with DR = 9 also exhibited fine dispersion with domains that were 30–60 nm in diameter [Fig. 6(c)]. This is also consistent with the XRD data shown in Figure 2.

More direct evidence of the formation of a true nanocomposite can be provided by TEM of ultramicrotomed sections. Figures 7–10 show TEM photographs of PTT hybrid fibers with various amounts of organoclay. The dark lines in the photograph are the intersections of the 1-nm-thick clay sheets, and the spaces between the dark lines are interlayer spaces.

Some of the clay layers in Figures 7 and 8 exhibit individual dispersion of delaminated sheets in the matrix, as well as regions where the regular stacking arrangement is maintained with a layer of polymer between the sheets. For PTT hybrid fibers containing organoclay at 1 and 3 wt % [Figs. 7(b) and 8(b)], some of the clay is well dispersed in the PTT matrix and some appears in agglomerations of $\sim$ 20 nm.

Typical TEM photographs for PTT hybrid fibers containing 2 and 4 wt % C_{12}PPh-MMT content are shown in Figures 9 and 10, respectively. Figure 9 shows that the organoclay was well dispersed in the polymer matrix at all magnification levels, although some particles were agglomerated. The presence of peaks in the XRD patterns of these samples can be attributed to these agglomerated layers (Fig. 1). For the 4 wt % hybrid fiber [Fig. 10(a,b)], some of the clay was well dispersed within the PTT matrix, while the remainder appeared in agglomerations larger than $\sim$ 10 nm. Unlike the hybrids containing IMD-MMT, the clay layers of the C_{12}PPh-MMT hybrid fiber (Figs. 9 and 10) were more dispersed into the matrix polymer. This difference in the clay dispersion might be attributed to the similarity of the chemical structure of organoclay and to the interactions between the organic part and the polymer matrix.

XRD, SEM, and TEM indicate that, for a low clay content, the clay particles were well dispersed throughout the PTT matrix; whereas agglomerated structures were evident at a higher clay content. The unusual thermomechanical properties of these nanocomposites are discussed in the following sections with reference to the homogeneous dispersion of the silicate nanoscale particles.

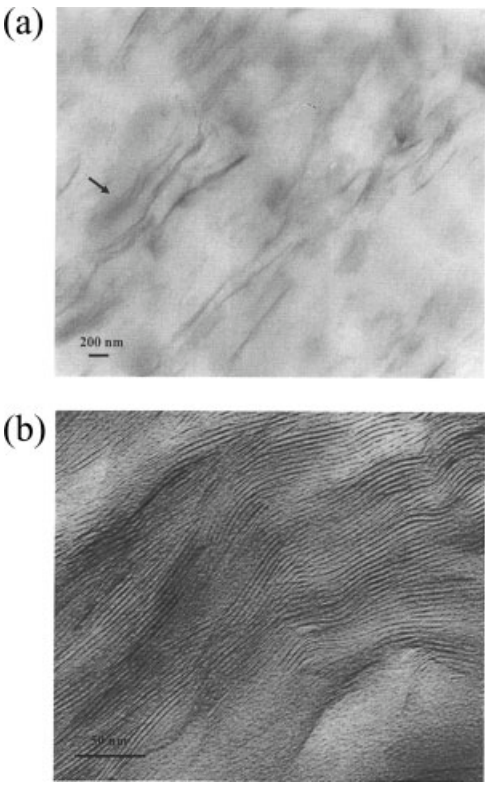

Figure 9 TEM micrographs of 2 wt % C_{12}PPh-MMT in PTT hybrid fiber at two different magnification levels.

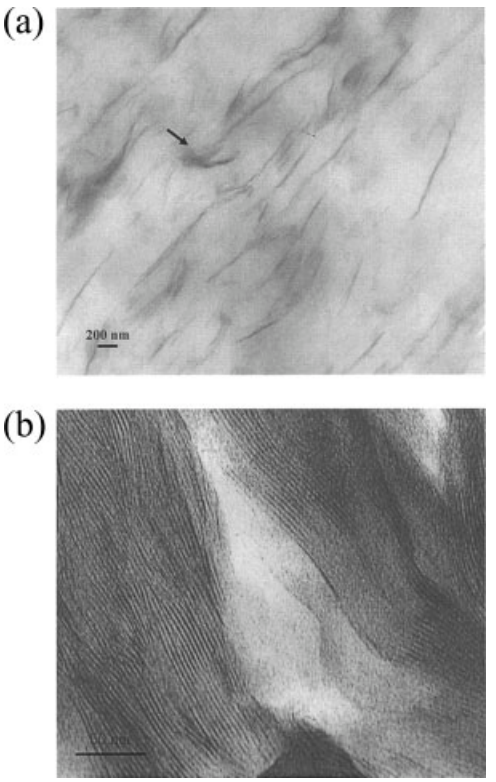

Figure 10 TEM micrographs of 4 wt % C_{12}PPh-MMT in PTT hybrid fiber at two different magnification levels.

Thermal behavior

The thermal properties of pure PTT and PTT hybrid fibers with different DRs are listed in Table I. The endothermic peak of pure PTT appeared at 228°C, which corresponds to the melting transition temperature (T_m). The maximum transition peaks in the DSC thermograms of the IMD-MMT/PTT hybrids increased from 228°C to 232°C as the organoclay content increased to 1 wt %, and then remained constant for an organoclay content up to 3 wt % (see Table I). This increase in T_m of the hybrids may be attributable to the thermal insulation effect of the clay layer structure, as well as from interactions between the organoclay and PTT molecular chains.[9,25] Compared with the results of IMD-MMT/PTT hybrids, the values of T_m remained fairly constant (i.e., varying from 227°C to 228°C) as the clay content increased from 0 to 4 wt % in C_{12}PPh-MMT hybrid fibers. This implies that varying the DR of the fiber during the extrusion did not result in a good insulation effect of the clays in the polymer matrix, as is evident in Table I.

Comparative TGA results for pure PTT and the PTT hybrids with 0–3 wt % IMD-MMT are also listed in Table I. The results in Table I indicate that the initial thermal degradation temperature (T_D^i) of the IMD-MMT/PTT hybrid fibers increased with the amount of organoclay. T_D^i for a 2% weight loss varied from 362°C to 372°C as the clay content increased from 0 to 3 wt % in the PTT hybrids; the largest increase in the initial thermal degradation temperature with respect to that of pure PTT was 6°C, for 3 wt % IMD-MMT/PTT. This increase in the thermal stability can be attributed to the high thermal stability of clay and to the interactions between the clay particles and the polymer matrix. The weight of the residue at 600°C increased from 1% to 11% as the clay content increased from 0% to 3%. This enhancement of char formation is ascribed to the high heat resistance of the clay.[26] Table I also presents the thermal stabilities of the C_{12}PPh-MMT hybrid fibers for various clay contents. T_D^i of the C_{12}PPh-MMT hybrid fibers increased from 362°C to 371°C for clay contents from 0 to 2 wt %, and then remained constant for a clay content up to 4 wt %.

The weight of the residue at 600°C (wt_R^{600}) for C_{12}PPh-MMT hybrids increased linearly from 1% to 12% as the clay content increased from 0 to 4 wt %. Table I indicates that the overall thermal properties of the PTT hybrid fibers with the two organoclays were virtually constant as DR increased from 1 to 9. The thermal stabilities of the PTT/organoclay hybrid fibers are plotted in Figure 11.

The above results show that introducing inorganic components into organic polymers can improve their thermal degradation stabilities. Clays exhibit good thermal stability because of the thermal insulation

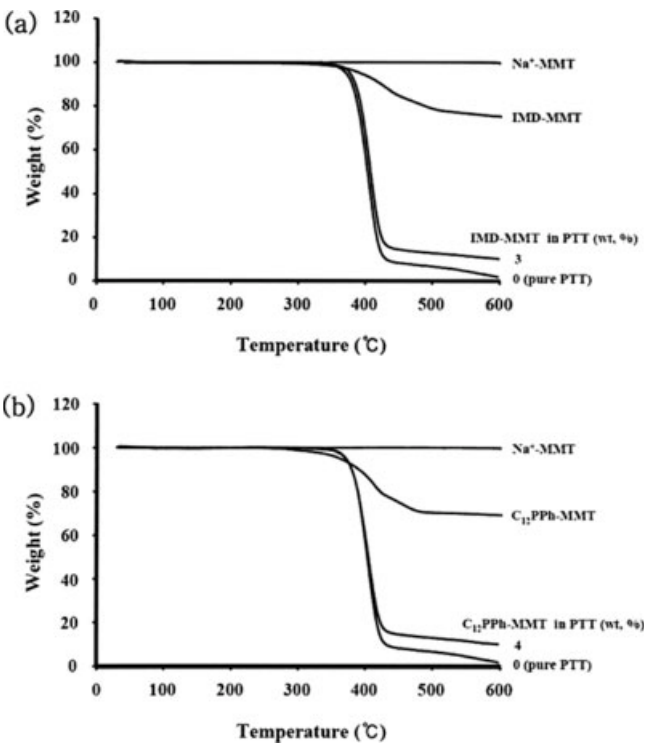

Figure 11 TGA thermograms of PTT hybrid fibers with (a) IMD-MMT and (b) C_{12}PPh-MMT contents.

effect of the clay layers and the mass-transport barrier they create to volatile products generated during decomposition.[27,28]

Tensile properties

The tensile properties of the IMD-MMT hybrid fibers are given in Table II. At DR = 1, the ultimate tensile strength of the IMD-MMT hybrid fibers increased with the amount of clay up to a certain value, and then remained constant. For example, the strength of 1 wt % PTT hybrid fibers was 44 MPa, which is about 40% higher than that of pure PTT (32 MPa); and was 45 MPa for 3 wt % organoclay. This plateauing of ultimate strength is mainly due to the ineffectual dispersion of clay particles when the content exceeded a certain threshold, as we have described previously.[10,27] Unlike the tensile strength, the initial modulus values increased linearly with increasing organoclay content. For a IMD-MMT content of 3 wt %, the modulus of the hybrid was 2.54 GPa, which is about 40% higher than that of pure PTT (1.77 GPa). This enhancement of the modulus is ascribed to the resistance exerted by the clay itself, as well as to the orientation and aspect ratio of the clay layers. Additionally, the enhanced stretching resistance of the oriented backbone of the polymer chain in the gallery also contributes to the enhancement of the modulus.

The tensile properties of the C_{12}PPh-MMT hybrid fibers are also given in Table II. These improved with increasing amounts of organoclay at DR = 1: when the organoclay content in the hybrids increased from 0 to 4 wt %, the ultimate tensile strength increased linearly from 32 to 48 MPa. For example, the ultimate strength of the hybrid fiber containing 4 wt % C_{12}PPh-MMT was 50% higher than that of a pure PTT fiber.

The same kind of behavior was observed for the initial moduli. For example, the initial tensile modulus of the fiber with 3 wt % organoclay was 2.76 GPa, which is about 50% higher than the modulus of pure PTT. For an organoclay content in PTT of 4 wt %, the modulus was about 70% higher (3.09 GPa) than that of pure PTT. This large improvement in tensile properties can be attributed to the interactions between PTT molecules and the layered organoclays, as well as to the rigid nature of the clay layers. Since clay is much more rigid than PTT molecules, the tensile properties of pure PTT are improved by hybridization and in particular because the organoclay layers are dispersed and intercalated in the PTT matrix. Many studies have found that nanocomposites exhibit significant improvements in ultimate strength and initial modulus as the organoclay content increases.[29–31]

The ultimate strengths of the IMD-MMT hybrid fibers containing 1–3 wt % organoclay were independent of DR in the range from 1 to 9. However, the initial modulus for the IMD-MMT hybrid fibers increased linearly with increasing DR. For example, the initial tensile modulus for a hybrid fiber with an IMD-MMT content of 1 wt % increased from 2.43 to 2.65 GPa as the DR increased from 1 to 9. When the organoclay content in PTT was 3 wt % at DR = 9, the

TABLE II
Tensile Properties of PTT Hybrid Fibers

Organoclay (wt %)	DR[a]	IMD-MMT			C_{12}PPh-MMT		
		Ult. Str. (MPa)	Ini. Mod. (GPa)	E.B.[b] (%)	Ult. Str. (MPa)	Ini. Mod. (GPa)	E.B. (%)
0 (pure PTT)	1	32	1.77	2	32	1.77	2
	3	35	1.85	2	35	1.85	2
	7	35	1.94	2	35	1.94	2
	9	34	2.02	3	34	2.02	3
1	1	44	2.43	2			
	3	48	2.57	2			
	7	46	2.60	2			
	9	47	2.65	2			
2	1	45	2.46	2	43	2.61	2
	3	45	2.54	2	40	2.58	2
	7	48	2.59	3	41	2.54	2
	9	46	2.70	2	41	2.57	2
3	1	45	2.54	2	45	2.76	3
	3	46	2.65	3	45	2.74	2
	7	47	2.84	2	38	2.75	2
	9	47	2.83	3	38	2.74	2
4	1				48	3.09	2
	3				46	3.10	3
	7				40	3.09	3
	9				41	3.04	2

[a] Draw ratio.
[b] Elongation percent at break.

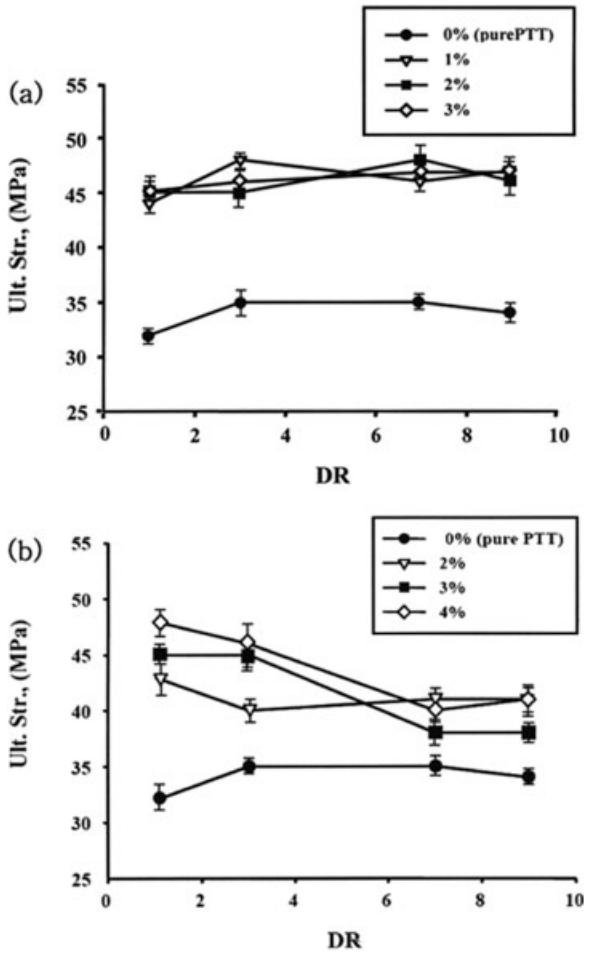

Figure 12 Effects of draw ratio on the ultimate tensile strength of (a) IMD-MMT and (b) C_{12}PPh-MMT contents.

modulus was about 40% higher (2.83 GPa) than that of pure PTT (2.02 GPa) at the same DR value.

For the C_{12}PPh-MMT hybrid fibers, both the ultimate strength and the initial modulus of the hybrid fibers decreased slightly with increasing DR, as is evident in Table II. For example, for a hybrid fiber with a C_{12}PPh-MMT content of 2 wt %, increasing DR from 1 to 9 decreased the tensile strength and initial modulus from 43 to 41 MPa and from 2.61 to 2.57 GPa, respectively. Similar trends were observed for hybrid fibers with C_{12}PPh-MMT contents of 3 and 4 wt %. The variations of the ultimate strengths and initial moduli of the PTT/organoclay hybrids are plotted against DR in Figures 12 and 13.

An increase in the tensile strength with increasing DR is very common in engineering plastics, and is usually observed for flexible coil-like polymers.[32,33] However, C_{12}PPh-MMT hybrid system did not follow this trend. The observed decline in the tensile properties seems to be the result of debonding between the organoclay and the matrix polymer, and the presence of many nanosized voids due to excessive stretching of the fibers. Because of imperfect bonding, debonding occurs at the interface, giving rise to a constant interfacial shear stress when strain is applied to the composite. The debonding at the polymer–clay interface at the point of fracture appears to promote some closure forces around the wake of a crack, which produces the observed crack growth resistance. Many studies have shown that an imperfect incursion/matrix interface cannot sustain the large interfacial shear stress that results from an applied strain.[34–36] This indicates that hydrostatic elongation during extrusion and compression molding operations results in debonding in the polymer chain as well as in the formation of voids around the polymer–clay interfaces.

The elongation at breakage of the IMD-MMT and C_{12}PPh-MMT hybrids was virtually independent of DR, changing from 2% to 3% as DR was increased from 1 to 9. This result is characteristic of materials reinforced with stiff inorganic materials, and is indicative of an intercalated morphology.

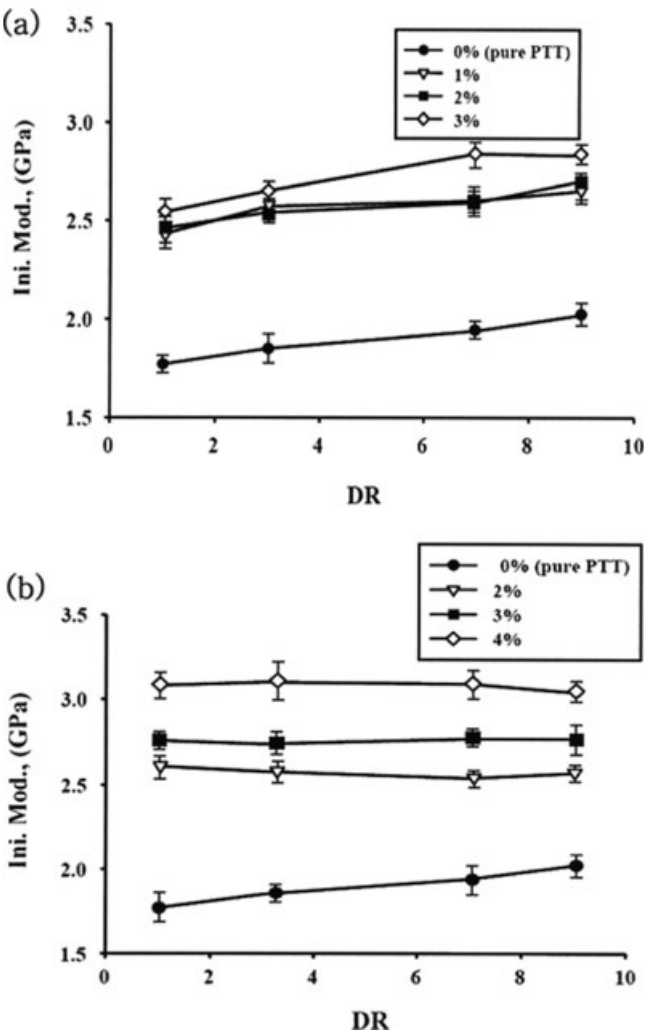

Figure 13 Effects of draw ratio on the initial tensile modulus of (a) IMD-MMT and (b) C_{12}PPh-MMT contents.

CONCLUSIONS

The thermomechanical properties and morphologies of new PTT nanocomposite fibers comprising two types of organoclay, IMD-MMT and C_{12}PPh-MMT, were determined. PTT hybrid fibers were synthesized using an *in situ* interlayer polymerization method with different organoclay contents. We found that the thermomechanical properties were dependent on both the type and amount of organoclay in the polymer matrix.

XRD, SEM, and TEM revealed that the morphology at a low organoclay content comprises a mixture of intercalated and partially exfoliated features. Each clay displayed well-dispersed individual clay layers in the PTT matrix, although some particles appeared in agglomerations larger than $\sim$ 20 nm. The dispersion was better when the amount of organoclay was lower.

The ultimate strength and initial modulus of the IMD-MMT hybrid fibers increased slightly as DR increased from 1 to 9, whereas those of the C_{12}PPh-MMT hybrid fibers decreased slightly with increasing DR. The observed decline in the tensile properties appears to be the result of debonding between the organoclay and the matrix polymer, and the presence of many nanosized voids due to excessive stretching of the fibers.

In summary, the addition of small amounts of organoclays to PTT was found to affect the thermal behavior and tensile mechanical properties of polymer/clay hybrid fibers.

References

1. Chang, J. H.; An, Y. U.; Sur, G. S. J Polym Sci Part B: Polym Phys 2003, 41, 94.
2. Osman, M. A.; Mittal, V.; Morbidelli, M.; Suter, U. W. Macromolecules 2003, 36, 9851.
3. Bharadwaj, R. K. Macromolecules 2001, 34, 9189.
4. Liang, Z.-M.; Yin, J. J Appl Polym Sci 2003, 90, 1857.
5. Ishida, H.; Campbell, S.; Blackwell, J. Chem Mater 2000, 12, 1260.
6. Itagaki, T.; Komori, Y.; Kuroda, K. J Mater Chem 2001, 11, 3291.
7. Hwang, S. H.; Paeng, S. W.; Kim, J. Y.; Huh, W. Polym Bull 2003, 49, 329.
8. Wang, D.; Zhu, J.; Yao, Q.; Wilkie, C. A. Chem Mater 2002, 14, 3837.
9. LeBaron, P. C.; Wang, Z.; Pinnavaia, T. J Appl Clay Sci 1999, 12, 11.
10. Chang, J.-H.; Kim, S. J.; Joo, Y. L.; Im, S. Polymer 2004, 45, 919.
11. Whinfield, J. R.; Dickson, J. T. Brit. Pat. 578,079 (1941).
12. Whinfield, J. R.; Dickson, J. T. U.S. Pat. 2,465,319 (1949).
13. Ward, I. M.; Wilding, M. A. Polymer 1977, 18, 327.
14. Desborough, I. J.; Hall, I. H.; Neisser, J. Z. Polymer 1979, 20, 545.
15. Huang, J. M.; Chang, F. C. J Polym Sci Part B: Polym Phys 2000, 38, 934.
16. Chen, K.; Shen, J.; Tang, X. J Appl Polym Sci 2005, 97, 705.
17. Zhu, J.; Morgan, A. B.; Lamelas, F. J.; Wilkie, C. A. Chem Mater 2001, 13, 3774.
18. Zhu, J.; Uhl, F. M.; Morgan, A. B.; Wilkie, C. A. Chem Mater 2001, 13, 4649.
19. Saujanya, C.; Imai, Y.; Tateyama, H. Polym Bull 2002, 49, 69.
20. Davis, C. H.; Mathias, L. J.; Gilman, J. W.; Schiraldi, D. A.; Shields, J. R.; Trulove, P.; Sutto, T. E.; Delong, H. C. J Polym Sci Part B: Polym Phys 2002, 40, 2661.
21. Ke, Y.; Lu, J.; Yi, X.; Zhao, J.; Qi, Z. J Appl Polym Sci 2000, 78, 808.
22. Zilig, C.; Mulhaupt, R.; Finter, J. Macromol Chem Phys 1999, 200, 661.
23. Dagani, R. Chem Eng News 1999, 77, 25.
24. Danumah, C.; Bousmina, M.; Kaliaguine, S. Macromolecules 2003, 36, 8208.
25. Hussain, M.; Varley, R. J.; Mathys, Z.; Cheng, Y. B.; Simon, G. P. J Appl Polym Sci 2004, 91, 1233.
26. Wen, J.; Wikes, G. L. Chem Mater 1996, 8, 1667.
27. Chang, J.-H.; Seo, B. S.; Hwang, D. H. Polymer 2002, 43, 2969.
28. Fornes, T. D.; Yoon, P. J.; Hunter, D. L.; Keskkula, H.; Paul, D. R. Polymer 2002, 43, 5915.
29. Yano, K.; Usuki, A.; Okada, A. J Polym Sci Part A: Polym Chem 1997, 35, 2289.
30. Lan, T.; Pinnavaia, T. J. Chem Mater 1994, 6, 2216.
31. Masenelli-Varlot, K.; Reynaud, E.; Vigier, G.; Varlet, J. J Polym Sci Part B: Polym Phys 2002, 40, 272.
32. La Mantia, F. P.; Valenza, A.; Paci, M.; Magagnini, P. L. J Appl Polym Sci 1989, 38, 583.
33. Chang, J.-H.; Jo, B. W. J Appl Polym Sci 1996, 60, 939.
34. Chawla, K. K. Composite Materials Science and Engineering; Springer: New York, 1987.
35. Curtin, W. A. J Am Ceram Soc 1991, 74, 2837.
36. Shia, D.; Hui, Y.; Burnside, S. D.; Giannelis, E. P. Polym Eng Sci 1987, 27, 887.